Watkins *et al. Retrovirology (2015) 12:61*
DOI 10.1186/s12977-015-0187-z

RETROVIROLOGY

RESEARCH

Open Access

In vivo analysis of Nef's role in HIV-1 replication, systemic T cell activation and CD4$^+$ T cell loss

Richard L Watkins, John L Foster* and J Victor Garcia*

Background: Nef is a multifunctional HIV-1 protein critical for progression to AIDS. Humans infected with *nef*(−) HIV-1 have greatly delayed or no disease consequences. We have contrasted *nef*(−) and *nef*(+) infection of BLT humanized mice to better characterize Nef's pathogenic effects.

Results: Mice were inoculated with CCR5-tropic HIV-1_{JRCSF} (JRCSF) or JRCSF with an irreversibly inactivated *nef* (JRCSFNef*dd*). In peripheral blood (PB), JRCSF exhibited high levels of viral RNA (peak viral loads of $4.71 \times 10^6 \pm 1.23 \times 10^6$ copies/ml) and a progressive, 75% loss of CD4$^+$ T cells over 17 weeks. Similar losses were observed in CD4$^+$ T cells from bone marrow, spleen, lymph node, lung and liver but thymocytes were not significantly decreased. JRCSFNef*dd* also had high peak viral loads ($2.31 \times 10^6 \pm 1.67 \times 10^6$) but induced no loss of PB CD4$^+$ T cells. In organs, JRCSFNef*dd* produced small, but significant, reductions in CD4$^+$ T cell levels and did not affect the level of thymocytes. Uninfected mice have low levels of HLA-DR$^+$CD38$^+$CD8$^+$ T cells in blood (1–2%). Six weeks post inoculation, JRCSF infection resulted in significantly elevated levels of activated CD8$^+$ T cells ($6.37 \pm 1.07\%$). T cell activation coincided with PB CD4$^+$ T cell loss which suggests a common Nef-dependent mechanism. At 12 weeks, in JRCSF infected animals PB T cell activation sharply increased to $19.7 \pm 2.9\%$ then subsided to $5.4 \pm 1.4\%$ at 14 weeks. HLA-DR$^+$CD38$^+$CD8$^+$ T cell levels in JRCSFNef*dd* infected mice did not rise above 1–2% despite sustained high levels of viremia. Interestingly, we also noted that in mice engrafted with human tissue expressing a putative protective HLA-B allele (B42:01), JRCSFNef*dd* exhibited a substantial (200-fold) reduced viral load compared to JRCSF.

Conclusions: Nef expression was necessary for both systemic T cell activation and substantial CD4$^+$ T cell loss from blood and tissues. JRCSFNef*dd* infection did not activate CD8$^+$ T cells or reduce the level of CD4$^+$ T cells in blood but did result in a small Nef-independent decrease in CD4$^+$ T cells in organs. These observations strongly support the conclusion that viral pathogenicity is mostly driven by Nef. We also observed for the first time substantial host-specific suppression of HIV-1 replication in a small animal infection model.

Keywords: HIV-1, Nef, Replication, Pathogenesis

Background

In individuals infected with *nef*-defective HIV-1, viral replication and pathogenesis were strongly attenuated [1–4]. Nef is a multifunctional protein and considerable effort has been made to understand which Nef activities are important for its contribution to AIDS [5–9]. These include the killing of bystander cells, maintenance of chronic viral replication leading to systemic immune system activation and blunting the host immune response [2, 10–16]. Ex vivo and in vivo models of HIV-1 infection have resulted in important advances defining Nef's critical role for high levels of viral replication and for CD4$^+$ T cell and thymocyte killing. Infection models include PBMCs, human fetal thymus organ culture, SCID-hu Thy/Liv mice and human aggregate lymphoid tissue explant from tonsil [17–26]. Unfortunately, these models could not address the systemic effects of Nef.

The bone marrow/liver/thymus (BLT) humanized mouse model has recently been employed to investigate

*Correspondence: john_foster@med.unc.edu; victor_garcia@med.unc.edu
Division of Infectious Diseases, UNC Center for AIDS Research, Genetic Medicine, University of North Carolina, Campus Box 7042, Chapel Hill, NC 27599-7042, USA

systemic effects of HIV-1 infection. In particular, BLT humanized mice have been inoculated with HIV-1_{JRCSF} (JRCSF) that has the CCR5 tropism predominantly found in infected individuals [27]. Denton et al. found high levels of replication by JRSCF and a significant cytopathic effect on $CD4^+CCR5^+$ T cells. Nie et al. [28] also found high levels of viral replication and targeted killing of $CD4^+CCR5^+$ T cells in NOG-hCD34 mice. Finally, Dudek et al. [29] also reported high levels of JRCSF replication in NOD/SCID BLT and NOD/SCID/IL2R$\gamma c^{-/-}$ BLT mice. However, the role of Nef in HIV replication and $CD4^+$ T cell depletion in the context of a CCR5-tropic virus has not been reported. In addition, Long et al. [30] infected BLT mice with JRCSF and observed systemic activation of peripheral blood $CD8^+$ T cells but the role of Nef was not investigated. Therefore, we have extended previous studies to compare JRCSF infection with infection by JRCSF modified to contain an irreversibly inactivated *nef* (JRCSFNef*dd*). In BLT humanized mice, Nef was found to have a limited role in JRCSF replication, but was necessary for systemic T cell activation and $CD4^+$ T cell loss in peripheral blood and in tissues. This was the case for multiple BLT mouse human tissue cohorts. However, in one exceptional cohort expressing an HIV-1 protective HLA-B allele (B42:01), the absence of Nef expression led to a 200-fold reduction in viral loads. This reduction was not observed in mice infected with the wildtype virus expressing Nef. This is the first demonstration of a host specific effect on viral load in an HIV-1 infection model.

Results

Infection of BLT humanized mice with JRCSF and JRCSFNef*dd*

We compared the infection of humanized BLT mice with the CCR5-tropic JRCSF and JRCSF with an irreversibly inactivated *nef* (JRCSFNef*dd*) to discern the phenotypic differences between wild type and *nef*(−) virus (Figure 1a). The deletions were made to reflect the truncations of *nef* found in patients reported to have been infected with a *nef*(−) virus [1, 3, 31, 32]. Though the proviral clone for JRCSFNef*dd* did not express Nef it did produce wild type levels of Env (Figure 1b). Further, in Figure 1c we observed that the *nef* deletions did not affect viral replication of this virus [33].

In Figure 2a, the levels of virus in blood following intravenous injection of JRCSF or JRCSFNef*dd* [9×10^4 tissue culture infectious units (TCIU)] were monitored for 17 weeks. Both viruses showed rapid increases of viral RNA in blood with high levels of virus throughout the course of infection. Peak viral loads for the two viruses were not significantly different (JRCSF, $4.71 \times 10^6 \pm 1.23 \times 10^6$ copies of viral RNA per ml versus JRCSFNef*dd*, $2.31 \times 10^6 \pm 1.67 \times 10^6$). However, at 8 weeks the average viral load for JRCSFNef*dd* mice was lower than the average viral load for JRCSF mice ($0.18 \times 10^6 \pm 0.09 \times 10^6$ and $1.24 \times 10^6 \pm 0.37 \times 10^6$, respectively; $p < 0.033$) but this significant difference was not observed at later time points because JRCSFNef*dd* viral loads displayed considerable variation over time (Additional file 1: Figure S1).

We also monitored $CD4^+$ T cells in blood post JRCSF inoculation over the course of infection. Our results show a slow, 17 week decline in $CD4^+$ T cells while $CD4^+$ T cell levels in uninfected mice remained unchanged (Figure 2b). These slow losses in $CD4^+$ T cells are in contrast with those previously reported with X4-tropic HIV-1_{LAI} (LAI) that rapidly depleted $CD4^+$ T cells from blood following inoculation [32]. Conversely, JRCSFNef*dd* infected BLT mice showed no reduction in peripheral blood $CD4^+$ T cells (Figure 2b) which is similar to what was previously observed during the course of LAINef*dd* infection under similar experimental conditions [32].

$CD4^+$ T cell levels in tissues of mice infected with JRCSFNef*dd* are higher than those in BLT mice infected with JRCSF

The BLT mice from Figure 2 were sacrificed and $CD4^+$ T cells present in bone marrow, spleen, lymph node, lung and liver were analyzed by flow cytometry (Figure 3a). In JRCSF infected mice, all five organs exhibited significant drops in the levels of $CD4^+$ T cells. In four of five organs, the JRCSFNef*dd* infected mice also had reduced levels of $CD4^+$ T cells, the exception being spleen. However, the loss of $CD4^+$ T cells as a result of JRCSFNef*dd* infection was not as great as for JRCSF ($p < 0.05$ for bone marrow, spleen, lymph node, lung and liver, Figure 3a). In the case of $CD4^+CD8^+$ thymocytes, there was no significant reduction noted for JRCSF or JRCSFNef*dd* (Figure 3b). These results show that the $CD4^+$ T cell depletion observed during the course of JRCSF's infection is blunted in the absence of Nef expression.

Analysis of systemic T cell activation during the course of infection with JRCSF and JRCSFNef*dd*

JRCSF infected mice display a relatively slow decline in peripheral blood (PB) $CD4^+$ T cells but JRCSFNef*dd* infected mice did not lose these cells (Figure 2b). The possibility of an association of $CD4^+$ T cell loss with systemic T cell activation was investigated [30]. Representative flow cytometric analyses of HLA-$DR^+CD38^+CD8^+$ T cells in blood at 12 weeks are presented in Figure 4a. Levels of activated $CD8^+$ T cells were quite low in uninfected mice but greatly increased during JRCSF infection. In contrast, JRCSFNef*dd* infection had little effect on T cell activation despite peak viral loads that were not

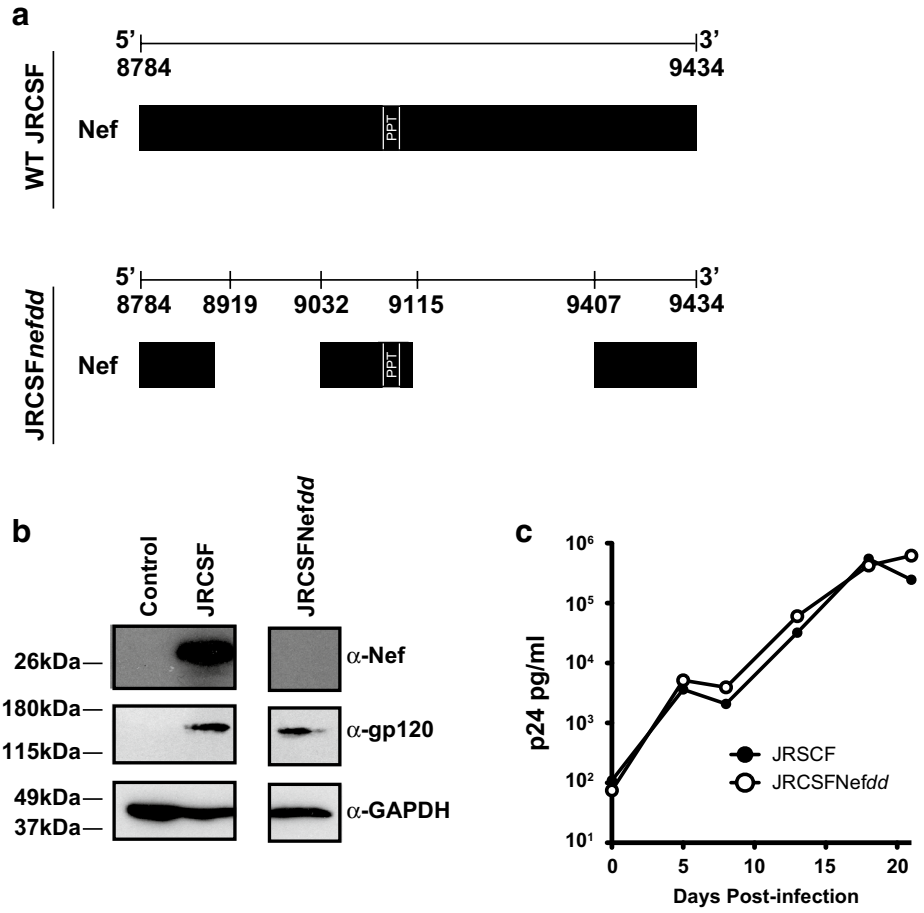

Figure 1 HIV-1_{JRCSF} with a truncated *nef*. **a** *Upper panel* schematic representation of wild type JRCSF *nef* (WT JRCSF) is presented. Nucleotides 8784–9434 in NCBI accession number, M38429, represent the *nef* coding sequence. *PPT* polypurine tract. *Lower panel*, a schematic presentation of *nef* with two deletions (JRCSFNef*dd*). A 114 bp deletion 5′ of the PPT from 8919 to 9032 inclusive was introduced into *nef*. The downstream sequence was shifted to the +1 reading frame by cutting with *Xho*I and filling in with Klenow ("Methods"). The 293 bp deletion 3′ of the PPT shifted downstream *nef* sequence to reading frame to +2. **b** The proviral clones for JRCSF and JRCSFNef*dd* were transfected into 293T cells and after 2 days Nef and Env expressions assessed by Western blots, GADPH is a loading control. **c** Replication competence of JRCSFNefdd was not diminished by loss of Nef as determined by $p24^{gag}$ production in CEM cells expressing CCR5. Cells were infected at 1×10^5 TCIU at an MOI 0.01 and the production of $p24^{gag}$ was followed for 21 days.

significantly lower than JRCSF (Figure 2a). In Figure 4b, the aggregate time courses for HLA-$DR^+CD38^+CD8^+$ T cells in blood are shown with individual plots presented in Additional file 2: Figure S2. Uninfected mice did not have elevated levels of activated $CD8^+$ T cells at any point during the experiment and JRCSFNef*dd* infected mice had nearly identical results with the exception of a single mouse (JRCSFNef*dd* 6) at a single time point (week 17) during the entire course of the study (Additional file 2: Figure S2). Interestingly, for JRCSF infected mice both the activation of $CD8^+$ T cells (JRCSF 6.3 ± 1.1% vs uninfected 1.7 ± 0.5%, p = 0.0095, p = 0.0008; Figure 4b) and the loss of PB $CD4^+$ T cells (JRCSF 6.4 ± 1.1% vs uninfected mice 0.6 ± 0.1%; p = 0.0095; Figure 2b) were first clearly evident at 6 weeks. T cell activation remained elevated and PB $CD4^+$ T cell continued to decline for 14 weeks (Figures 2b, 4b). Therefore, the appearance of activated $CD8^+$ T cells and loss of $CD4^+$ T cells in blood were tightly correlated. At 12 weeks, further activation occurred (JRCSF, 19.7 ± 2.9% HLA-$DR^+CD38^+CD8^+$ T cells versus uninfected, 1.1 ± 0.3%, p = 0.0003 and versus JRCSFNef*dd*, 1.7 ± 0.5% p = 0.0008). There was no dramatic effect of this spike on viral load or the steady decline in PB $CD4^+$ T cells (Figure 2a, b).

Time courses of T cell activation for the individual control or JRCSF and JRCSFNef*dd* infected mice are presented in Figure 5. In each JRCSF infected mouse, the early appearance of $CD8^+$ T cell activation is

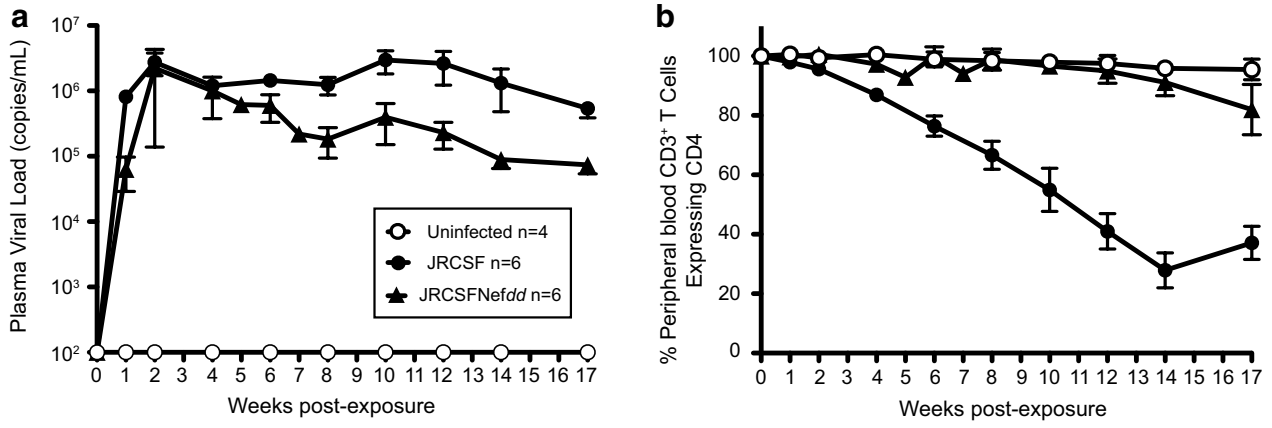

Figure 2 Viral load analysis and PB $CD4^+$ T cell loss in mice infected with JRCSF and JRCSFNef*dd*. **a** Viral loads (copies of viral RNA per ml of plasma) were plotted for BLT mice that were exposed to 90,000 TCIU. JRCSF, JRCSFNef*dd* and uninfected mice were followed for 17 weeks. **b** The percent of $CD4^+$ T cells out of total T cells in peripheral blood are plotted for the three groups of mice in **a**.

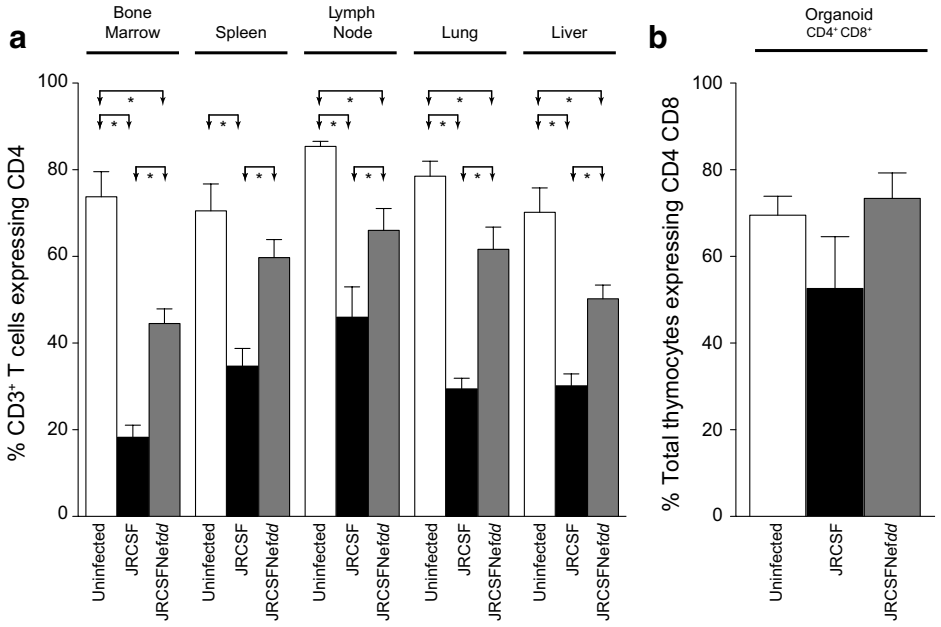

Figure 3 Systemic $CD4^+$ T cell but not thymocyte loss in mice infected with JRCSF and JRCSFNef*dd*. **a** $CD4^+$ T cell analysis was performed on five organs from un-exposed BLT mice (uninfected, n = 4), JRCSF infected BLT mice (n = 5) and JRCSFNef*dd* infected BLT mice (n = 6). Significant differences are indicated by *lines* and *arrows* above respective bars (*$p < 0.05$). **b** The same analysis as in **a** is presented for $CD4^+CD8^+$ double positive thymocytes relative to total thymocytes. No statistical differences were observed. *Error bars* are the mean ± SEM.

temporally associated with the initial loss of $CD4^+$ T cells in blood. Conversely, there was no elevation of $HLA\text{-}DR^+CD38^+CD8^+$ T cells and no loss of $CD4^+$ T cells in PB for either uninfected or JRCSFNef*dd*-infected BLT mice except as noted above for JRCSFNef*dd* 6 at 17 weeks. At this singular, late time point, the association between T cell activation and $CD4^+$ T cell decline is maintained despite the absence of Nef expression (Additional file 2: Figure S2). In sum, our results demonstrate a strong and highly consistent linkage of $CD8^+$ T cell activation to the loss of PB $CD4^+$ T cells in JRCSF infected mice.

Specific suppressive effect on JRCSFNef*dd* viral load in mice reconstituted with cells and tissue expressing HLA B42:01

Dudek et al. investigated infection with JRCSF of eight BLT humanized mice tissue cohorts with many HLA

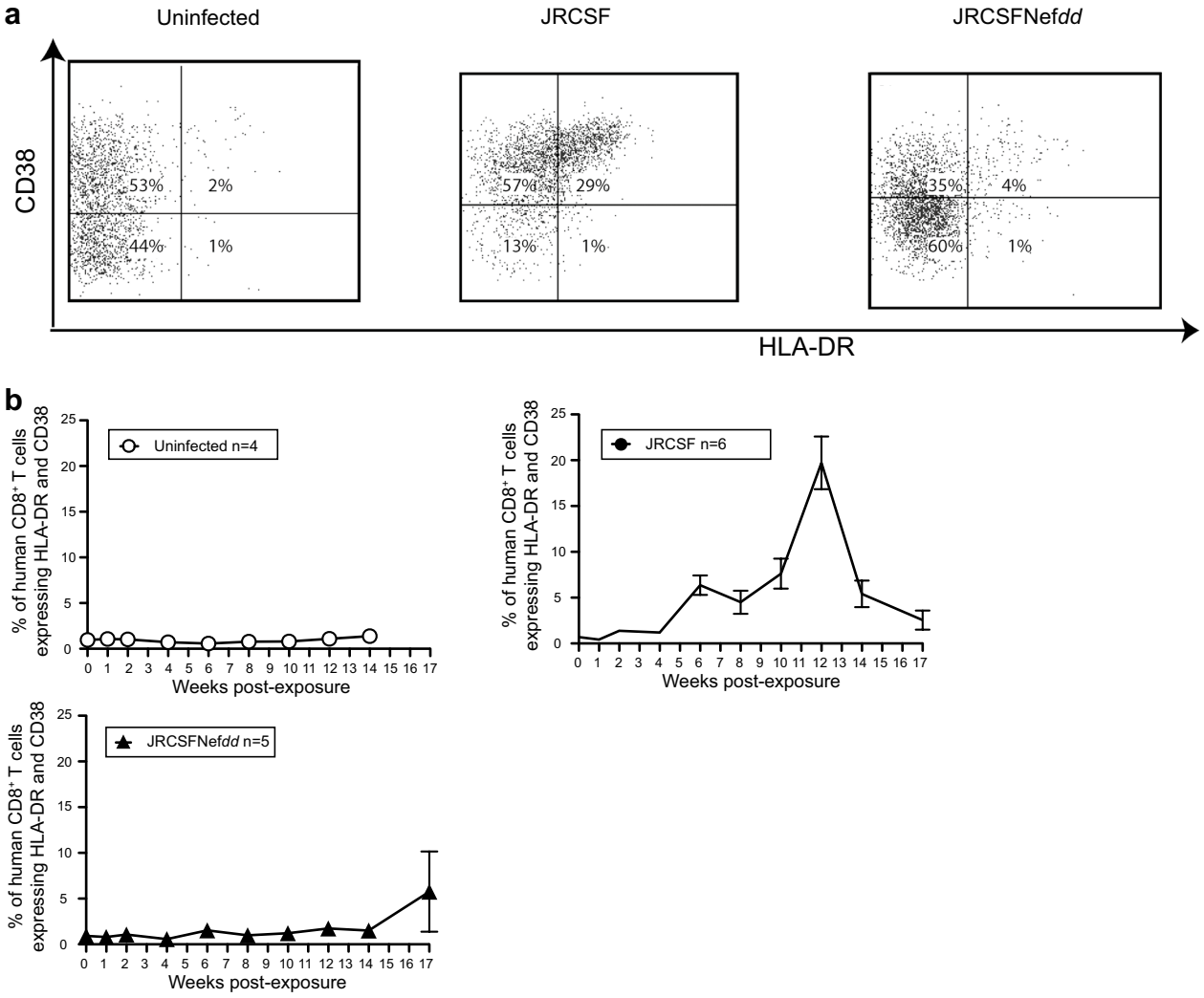

Figure 4 Systemic T cell activation during infection with JRCSF and JRCSFNef*dd*. Systemic T cell activation was assessed by the levels of HLA-DR$^+$CD38$^+$CD8$^+$ relative to total CD8$^+$ T cells in blood. **a** Representative *dot plots* for the presence of activated CD8$^+$ T cells in blood of uninfected, JRCSF-infected (JRCSF 1) and JRCSFNef*dd*-infected (JRCSFNef*dd* 6) mice. Gating protocol was performed as indicated in "Methods". Data shown are from 12 wpi. **b** Aggregate data of CD8$^+$ T cell activation over the course of 17 weeks of infection is shown for uninfected (n = 4), JRCSF infected (n = 6) and JRCSFNef*dd* infected (n = 5) mice.

haplotypes represented. The only cohort-specific reduction in viral load found was with mice implanted with B57-expressing human tissue. Mice with human cells expressing this protective haplotype exhibited a four-fold reduction in viral load relative to all other haplotypes investigated including the protective allele, B27 [29]. We did not have tissue with the B57 haplotype and consistent with Dudek et al. we observed no cohort-specific suppression of viral load with JRCSF infection. Nor did we observe reductions in viral loads with JRCSFNef*dd* infections except for one cohort of mice designated Cohort 1 (Table 1). Cohort 1 has HLA haplotypes, A23:01, A30:01, B42:01, B53:01, C08:01, C17:01. In a report based on a large population of South African HIV-1 positive individuals, B42:01 was one of the few HLA-B haplotypes found to have significantly lower viral loads [34]. Two Cohort 1 mice were infected with JRCSFNef*dd* and had consistently lower viral loads than two Cohort 1 JRCSF mice at every time point (Figure 6a). At week 10, this reduction reached 200-fold. Comparisons of the four JRCSF and four JRCSFNef*dd* mice from Cohorts 2, 3, 4, and 5 gave considerable overlap in the viral loads with the JRCSF and JRCSFNef*dd* infected mice (Figure 6b). On the basis of these results, we hypothesize that JRCSFNef*dd* infected

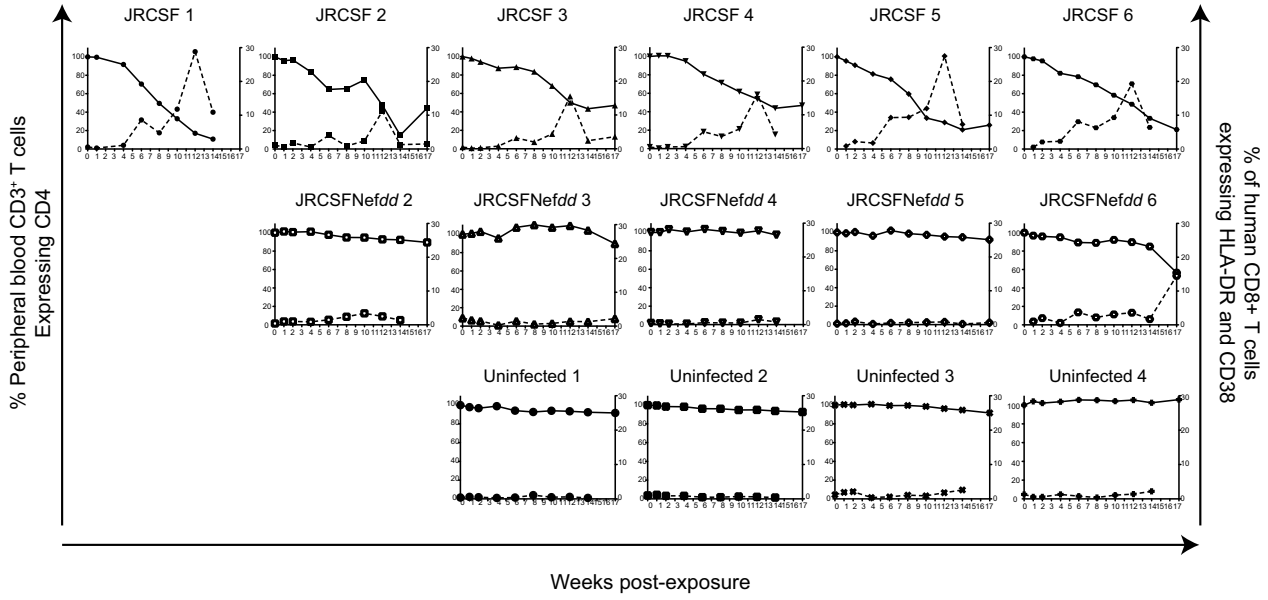

Figure 5 Systemic T cell activation is compared to PB $CD4^+$ T cell loss in individual mice. Plots for individual mice of $CD4^+$ T cells (*left y axis*) and of $HLA\text{-}DR^+CD38^+CD8^+$ T cells (*right y axis*) over the infection time course are shown. *Top row* all six JRCSF infected mice show increases in $CD8^+$ T cell activation concomitant to PB $CD4^+$ T cell loss. *Middle row* JRCSFNef*dd* infected BLT mice show very low T cell activation and no $CD4^+$ T cell loss except for JRCSFNef*dd* 6 which had a drop in $CD4^+$ at week 17. *Bottom row* uninfected mice show very low T cell activation and no $CD4^+$ T cell loss.

Table 1 Haplotype of tissues/CD34 stem cells used for the construction of the BLT humanized mice used

Cohort 1	A23:01 A30:01 B42:01 B53:01 C08:01 C17:01	JRCSF 3, 4; JRCSFNef*dd* 4, 5
Cohort 2	A02:01 A02:01 B35:17 B52:01 C03:03 C04:04	JRCSF 2; JRCSFNef*dd* 3
Cohort 3	A02:01 A03:01 B35:01 B44:02 C04:01 C05:01	JRCSF 1
Cohort 4	A11:01 A24:02 B35:01 B35:24 C04:01 C04:01	JRCSF 5, 6; JRCSFNef*dd* 6
Cohort 5	*A02:06* A34:01 B39:05 B40:02 C07:02 C15:02	JRCSFNef*dd* 2
Cohort 6	ND	JRCSFNef*dd* 1

Multiple BLT mice constructed from the same human tissue are designated by a cohort number. The lower level of PB JRCSFNef*dd* viral RNA compared to JRCSF viral RNA in Cohort 1, but none of the others, led us to have the MHCI haplotypes determined. A02:06 in Cohort 5 is in italics because it appears to be a previously undocumented A2 variant (similar to A*02:06). There is a nucleotide substitution in exon 3 that is not present in the HLA database. As it is located in exon 3 and encodes a non-synonymous substitution (Histidine > Leucine at codon 114), it may impact peptide binding.

mice can have substantially reduced viral burdens relative to JRCSF mice but the reduction is dependent on the genotype of the engrafted tissue.

Disscusion

We have extensively characterized infection of BLT humanized mice with a wild type R5-tropic virus (JRCSF) and an isogenic *nef*(−) virus (JRCSFNef*dd*). Following JRCSF infection, there is a progressive 17 week decline in $CD4^+$ T cells in blood to about 25% of the levels found in uninfected mice. Also at 17 weeks, $CD4^+$ T cells in organs were reduced to 20–40% of the levels in uninfected mice. These substantial pathogenic effects are, nonetheless, less aggressive than the $CD4^+$ T cell losses previously reported for the CXCR4-tropic HIV-1 LAI in this same model and under similar experimental conditions [32]. However, one stark difference between JRCSF and LAI infection was that thymocytes were present at near normal levels throughout JRCSF infection but massively depleted by LAI. The maintenance of thymocyte viability despite R5-tropic infection may reflect the paucity of CCR5 expressing cells in thymocytes [27]. Interestingly, Jamieson et al. [24] reported severe losses of thymic organoid cells with X4-tropic NL-43 infection of SCID–hu mice but little evidence of pathogenicty for R5-tropic JRCSF. Not surprisingly, our results reflect these earlier results with regard to thymocytes. However, previously unreported is the loss of about 75% of $CD4^+$ T cells from blood and tissues. In contrast to the rapid loss of $CD4^+$ T cells in BLT mice with LAI infection, a largely intact human thymic organ during JRCSF infection could replenish $CD4^+$ T cells in the periphery and slow the net loss of $CD4^+$ T cells. The loss of thymocytes during X4-tropic LAI infection would not allow buffering the $CD4^+$ T cell levels in tissues resulting in dramatic depletion of these cells [32]. These considerations suggest

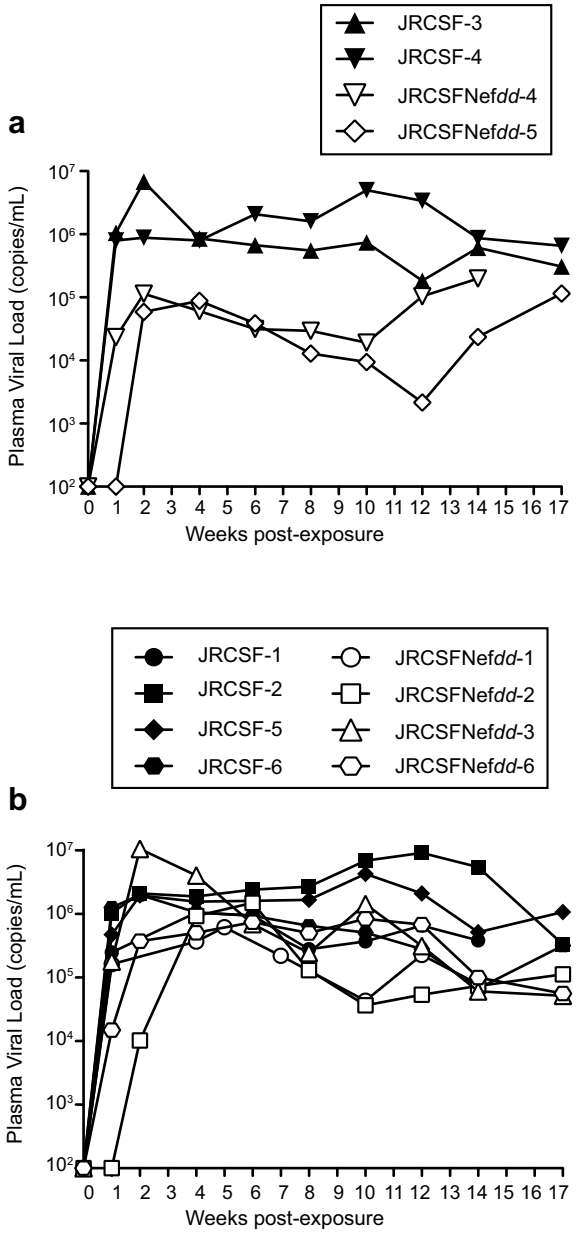

Figure 6 Viral load time courses for JRCSFNef*dd* infected mice and JRCSF infected mice with Cohort 1 tissue. **a** The data in Figure 2a is re-plotted to separate the four Cohort 1 mice from the other eight mice. Two Cohort 1 mice were infected with JRCSF and two were infected with JRCSFNef*dd*. **b** The remaining eight mice were plotted. These mice were from Cohorts 2–5; see Table 1).

that R5-tropic infection may be inherently as cytotoxic as X4-tropic infection but exhibits less drastic effects because of different cellular targets.

Another difference between LAI and JRCSF infection was that peak viral loads were reduced about sevenfold with LAINef*dd* infection compared to wild type but a only a twofold reduction in peak viral load was noted with JRCSFNef*dd* (Figure 2), [32]. HIV-1 $_{JRFL}$ (JRFL) is closely related to JRCSF and Usami and Gottlinger reported that JRFL and *nef*(−) JRFL have similar infectivities. The B-C hairpin of the V2 region fails to respond to Nef and prevents the functioning of Nef to enhance virion infectivity [35]. JRCSF has 90% identical residues in the B-C hairpin to JRFL which may account for the low impact of the loss of Nef expression on JRCSFNef*dd* peak viral load. However, arguing against this explanation for the small impact of *nef* inactivation on viral replication is that JRCSF replicated to high viral loads with or without *nef*.

The T cell activation data (Figures 4, 5) in combination with the T cell loss in tissues data (Figure 3a) for JRCSF and JRCSFNef*dd* gives evidence for two mechanisms of JRCSF cell toxicity. One mechanism observed with JRCSFNef*dd* infection is Nef and systemic T cell activation independent. It results in a relatively low level of killing and is only found in tissues as $CD4^+$ T cells in blood are not reduced. The second mechanism is Nef-dependent and may account for the parallel loss of $CD4^+$ T cells in blood and increased PB $CD8^+$ T cell activation. The higher level of killing in tissues by JRCSF is also likely to be the result of Nef expression and/or T cell activation (Figure 3a). Killing of $CD4^+$ T cells has been linked to systemic T cell activation [30] and we found a strong association of PB $CD4^+$ T cell loss with systemic T cell activation. Since PB $CD4^+$ T cells are not productively infected by HIV-1 the mechanism of PB $CD4^+$ T cell loss caused by JRCSF infection is likely to be indirect. Elevated $CD8^+$ T cell activation was first noted at 6 weeks when PB $CD4^+$ T cell have clearly begun to decline and continued to increase to very high levels by 12 weeks (Figure 2b, 4b). The expression of Nef was necessary for these effects as JRCSFNef*dd* failed to cause activation or $CD4^+$ T cell loss.

The percent of $CD4^+$ T cells that express CCR5 is relatively high in bone marrow, lung and liver and these cells are lost with JRCSF infection [27]. It is not known if the cytotoxic effect of JRCSF in these organs is indirect through systemic T cell activation or direct as a result of one or more of Nef's numerous activities. Direct Nef effects have been proposed for killing bystander cells by induction of apoptosis [14, 15, 36–39]. However, we also observed reduced but significant losses of $CD4^+$ T cells in tissues with JRCSFNef*dd* infection. To explain the loss of $CD4^+$ T cells in tissues following JRCSFNef*dd* infection, mechanisms that are independent of Nef and systemic T cell activation are required. One possibility involves pyroptotic death of abortively infected cells [40, 41]. In JRCSFNef*dd*-infected mice, the combined effects of having high peak viral loads in the absence of systemic T cell

activation may be expected to favor abortive infection. An alternate mechanism could be the direct binding to bystander cells by Env [42, 43]. The full elucidation of the mechanism of Nef- and activation-independent $CD4^+$ T cell loss will be important for complete understanding of $CD4^+$ T cell loss in R5-tropic HIV-1 infection. The ability of Nef to modulate cellular protein kinases may be critical in this regard [5, 38, 44, 45].

In general, we did not observe significant reductions in viral loads for JRCSFNef*dd* infected mice compared to JRCSF infected mice but there was a reduction of JRCSFNef*dd* viral load in BLT mice from one of six cohorts. Specifically, there was a 200-fold reduction of viral load in JRCSFNef*dd* infected mice compared to JRCSF infected mice sharing Cohort 1 reconstitution. The host factor responsible for the reduction in viral load has not been identified, however, B42:01 is one of the HLA haplotypes for Cohort 1 and B42:01 has a negative impact on viral loads of HIV-1 positive individuals [34]. The reduction in viral loads observed for the JRCSFNef*dd* infected Cohort 1 mice suggest the intriguing possibility that a weak anti-HIV effect by B42:01 in BLT mice is greatly enhanced when Nef is absent. The converse conclusion is that the all other haplotypes present in this study are ineffective in reducing viral load even with *nef*(−) virus. In future studies, it will be important to screen HLA haplotypes to determine the anti-viral effects of multiple HLA haplotypes, especially the well-known protective allele B57. In this regard, the Sydney Blood Bank Cohort of patients infected with *nef*(−) HIV-1 all had greatly delayed disease progression, however of special interest is patient C135 with the B57 haplotype that was negative for virus in blood for 29 years [46, 47].

Conclusions

We have demonstrated that in the context of the CCR5-tropic HIV-1 infection the accessory protein Nef is required for peripheral blood $CD4^+$ T cell depletion. In addition, we observed an association between peripheral blood $CD8^+$ T cell activation and the loss of $CD4^+$ T cells. Neither activation nor $CD4^+$ T cell loss was observed in mice infected with JRCSFNef*dd*. The requirement of Nef expression for $CD8^+$ T cell activation during of HIV-1 infection suggests that Nef plays a critical role in the widespread nature of HIV-1 cytotoxicity. Moreover, this Nef-dependent activation is linked to the loss of $CD4^+$ T cells but the mechanism is not known. A relatively small, Nef-independent cytotoxic T cell effect was also observed. This loss of $CD4^+$ T cells was restricted to tissues. The significance of this finding is unknown but overall pathogenicity appears to be largely driven by Nef. Future investigations will pursue understanding the long-elusive mechanism behind the fundamental phenomenon of $CD4^+$ T cell loss during HIV-1 infection.

We also observed a reduced ability of JRCSFNef*dd* to replicate in mice from a specific cohort of identical engrafted human tissue. Of great interest, this cohort expressed B42:01 which is an allele significantly associated with reduced viral burdens by studies of large populations of HIV-1 infected individuals. Thus, the BLT humanized mouse infected with JRCSFNef*dd* may provide a platform to independently identify protective HLA alleles.

Methods

Preparation of humanized BLT mice

Humanized BLT mice were prepared as previously described [27, 29, 30, 32, 48–55]. Briefly, thymus/liver implanted NOD/SCID IL-2$\gamma^{-/-}$ mice (The Jackson Laboratories, Bar Harbor, ME, USA) were transplanted with autologous human $CD34^+$ cells isolated from fetal liver (Advanced Bioscience Resources, Alameda, CA, USA). Reconstituted mice have a highly representative human immune system. Multiple mice reconstituted from a single source of autologous thymus/liver implant and human $CD34^+$ cells represent a single cohort. Mice from seven cohorts were used (Table 1). Human reconstitution in the peripheral blood of these mice was monitored periodically by flow cytometry prior to use (FACSCanto; BD Biosciences). Mice were maintained at the Division of Laboratory Animal Medicine, University of North Carolina at Chapel Hill (UNC-CH) in accordance with protocols approved by the UNC-CH Institutional Animal Care and Use Committee.

Cell lines and culture conditions

293T and TZM-bl cells were maintained in Dulbecco's modified Eagle's medium (DMEM; Cellgro, Herndon, VA, USA) supplemented with 10% fetal bovine serum (FBS; Cellgro), 100 IU/ml of penicillin, 100 μg/ml streptomycin, and 2 mM glutamine (Cellgro) in 10% CO_2 at 37°C.

Proviral clones

The proviral clone, pYK-JRCSF (accession #M38429), was described by Koyanagi et al. [56]. pYK-JRCSFNef*dd* was constructed by first creating a 5′ deletion upstream of the PPT. The *Xho*I/*Acc*65I fragment was removed and blunt ends were made with Klenow followed by religation. The reconstituted *Xho*I site was cut and treated with Klenow and religated. In the 3′ half of *nef* 288 bases were deleted by site directed mutagenesis as previously described for pLAInef*dd* [32].

Exposure of BLT humanized mice to JRCSF and JRCSFNef*dd*, assay of viral production, tissue harvesting and cytometric analyses

Stocks of JRCSF and JRCSFNef*dd* were prepared as previously described [44, 57]. Briefly, proviral clones were transfected into 293T cells. Viral supernatant was

collected 48 h after transfection and diluted in Dulbecco's modified Eagle's medium (DMEM) supplemented with 10% fetal bovine serum, 100 IU penicillin/ml, 100 μg/ml streptomycin, and 2 mM glutamine. TZM-bl cells were infected in 12-well tissue culture plates with 0.4 ml of virus at multiple dilutions in medium for 2 h. Then, 1.0 ml of supplemented DMEM was added and the plates incubated overnight. Virus containing medium was removed the next day, replaced with fresh DMEM plus 10% fetal bovine serum and the incubation continued for 24 h. The cells were fixed and stained with 5-bromo-4-chloro-3-indolyl-β-D-galactopyranoside (40 h after first exposure to virus). Blue cells were counted directly to determine infectious particles per mL. Each titer of these viral stocks was performed in triplicate and at least two different titer determinations were performed for each batch of virus. $p24^{gag}$ was determined for each virus preparation with the ELISA HIV-1 p24 antigen capture assay from Advanced Bioscience Laboratories Inc. (Cat. No. 5421).

Intravenous exposure of BLT mice with infectious virus was conducted via tail vein injection with indicated tissue culture infectious units (TCIU). Viral load in peripheral blood of infected mice was monitored longitudinally by quantitative real-time PCR using Taqman RNA to-C_T™ 1-step kit from Applied Biosystems, USA [50, 58]. The sequences of the forward and reverse primers and the Taqman probe for PCR were: 5′-CATGTTTTCAGCATTATCAGAAGGA-3′, 5′-TGCTTGATGTCCCCCCACT-3′, and 5′-FAM CCACCCCACAAGATTTAAACACCATGCTAA-Q-3′, respectively.

$CD4^+$ and $CD8^+$ T cell levels were monitored by flow cytometric analysis as previously described [27, 53, 55]. Immunophenotyping was performed on blood samples collected longitudinally and on mononuclear cells isolated from tissues at harvest. Whole peripheral blood (PB) from humanized mice was analyzed according to the BD Biosciences Lyse/Wash protocol (Cat. No. 349202) as we have previously described [59]. Briefly, following antibody labeling of whole blood, red blood cells were lysed. The remaining cells were washed, fixed and the sample was analyzed by flow cytometry. Tissue mononuclear cell isolations and immunophenotyping analyses were also performed according to published methods [27, 53, 55]. Flow cytometric gating for CD4 and CD8 cell surface expression was performed as follows: (step 1) forward and side scatter properties were utilized to set a live cell gate; (step 2) live cells were then analyzed for expression of the human pan-leukocyte marker CD45; (step 3) human leukocytes were then analyzed for hCD3 and (step 4) T cells or thymocytes were analyzed for hCD4 and hCD8 expression.

The panel of antibodies for analysis of $CD8^+$ T cells double positive for $CD38^+$ and $HLA\text{-}DR^+$ was CD8 FITC (SK1), HLA-DR, PE (TU36) or IgG2bκ PE, CD4 PerCP (SK3), CD3 PE-Cy7 (SK7), CD38 APC (HB7) or IgG1κ APC, and CD45 APC-Cy7 (2D1) (all purchased from BD Biosciences). Gating was performed as follows: (step 1) forward and side scatter properties were utilized to set a live cell gate; (step 2) live cells were then analyzed for expression of the human pan-leukocyte marker CD45; (step 3) human leukocytes were then analyzed for CD3; (step 4) T cells were analyzed for CD4 and/or CD8 expression; (step 5) activation of human $CD8^+$ T cells was analyzed for HLA-DR and CD38 expression [30]. Gates defining HLA-DR and CD38 expression were set with isotype-matched fluorophore-conjugated antibodies.

Viral replication in vitro

The human T cell line, CEM (NIH AIDS Reagent Program), was modified to express CCR5 [33]. Cells were infected with virus stocks at 1×10^5 TCUI at an MOI of 0.01 in complete RPMI containing 2 μg/ml polybrene at 37°C, 5% CO_2 for 4 h. The cells were washed extensively with PBS and cultured at 37°C, 5% CO_2 in complete RPMI. Cell cultures were passaged at 0, 5, 8, 13, 18, and 21 days post-infection and a sample of the culture supernatant was collected for quantification of viral capsid protein by $p24^{gag}$ ELISA.

HLA haplotyping

HLA haplotypes were determined by sequence based typing using SeCore HLA typing reagents (Life Technologies) on an ABI3500 capillary sequencer. Data analysis was performed using uType software (Life Technologies). When necessary, ambiguous allele combinations were resolved with sequence specific oligonucleotide probe hybridization (ThermoFisher). DNA was extracted a Promega Maxwell automated DNA extractor and kits.

Statistical analysis

Student t test was conducted using Prism Version 5 (Graph Pad). All data were plotted as mean ± SEM.

Additional files

Additional file 1: Figure S1. Viral loads plotted for individual mice **(A)**. The viral loads for each of the six BLT humanized mice infected with JRCSF from Figure 2A are plotted separately. **(B)** The viral loads for the six BLT humanized mice infected with JRCSFNef*dd* from Figure 2A are presented as individual plots. JRCSF infected mice are from four different cohorts and JRCSFNef*dd* infected mice are from five different cohorts. The cohorts were distributed as follows. Cohort 1—JRCSF 3, 4 and JRCSFNef*dd* 4,5; Cohort 2—JRCSF 2, and JRCSFNef*dd* 3; Cohort 3—JRCSF 1; Cohort 4—JRCSF 5, 6 and JRCSFNef*dd* 6; Cohort 5—JRCSFNef*dd* 2; Cohort 6—JRCSFNef*dd* 1.

Additional file 2: Figure S2. Time course of T cell activation plotted for individual mice. **(A)** Individual JRCSF infected mice are shown. **(B)** Individual JRCSFNef*dd* mice are shown.

Authors' contributions
RLW and JLF performed experiments. RLW, JLF and JVG designed experiments. RLW, JLF, and JVG analyzed the data. RLW, JLF and JVG wrote the manuscript. All authors read and approved the final manuscript.

Acknowledgements
This work was supported by Grant AI33331 from the National Institute of Allergy and Infectious Diseases of the National Institutes of Health, USA and UNC CFAR P30 A1504410. R. W. was supported in part by NIH Virology Training Grant 5T32A1007419. Haplotyping of tissue samples was performed by Dr. John Schmitz at the Immunology and Virology Core of the UNC CFAR.

Compliance with ethical guidelines

Competing interests
The authors declare that they have no competing interests.

Received: 18 May 2015 Accepted: 29 June 2015
Published online: 14 July 2015

References

1. Calugi G, Montella F, Favalli C, Benedetto A (2006) Entire genome of a strain of human immunodeficiency virus type 1 with a deletion of nef that was recovered 20 years after primary infection: large pool of proviruses with deletions of env. J Virol 80:11892–11896
2. Gorry PR, McPhee DA, Verity E, Dyer WB, Wesselingh SL, Learmont J et al (2007) Pathogenicity and immunogenicity of attenuated, nef-deleted HIV-1 strains in vivo. Retrovirology 4:66
3. Kirchhoff F, Greenough TC, Brettler DB, Sullivan JL, Desrosiers RC (1995) Brief report: absence of intact nef sequences in a long-term survivor with nonprogressive HIV-1 infection. N Engl J Med 332:228–232
4. Kondo M, Shima T, Nishizawa M, Sudo K, Iwamuro S, Okabe T et al (2005) Identification of attenuated variants of HIV-1 circulating recombinant form 01_AE that are associated with slow disease progression due to gross genetic alterations in the nef/long terminal repeat sequences. J Infect Dis 192:56–61
5. Abraham L, Fackler OT (2012) HIV-1 Nef: a multifaceted modulator of T cell receptor signaling. Cell Commun Signal 10:39
6. Arhel NJ, Kirchhoff F (2009) Implications of Nef: host cell interactions in viral persistence and progression to AIDS. Curr Top Microbiol Immunol 339:147–175
7. Foster JL, Denial SJ, Temple BR, Garcia JV (2011) Mechanisms of HIV-1 Nef function and intracellular signaling. J Neuroimmune Pharmacol 6:230–246
8. Kirchhoff F (2010) Immune evasion and counteraction of restriction factors by HIV-1 and other primate lentiviruses. Cell Host Microbe 8:55–67
9. Laguette N, Bregnard C, Benichou S, Basmaciogullari S (2010) Human immunodeficiency virus (HIV) type-1, HIV-2 and simian immunodeficiency virus Nef proteins. Mol Aspects Med 31:418–433
10. Jia X, Singh R, Homann S, Yang H, Guatelli J, Xiong Y (2012) Structural basis of evasion of cellular adaptive immunity by HIV-1 Nef. Nat Struct Mol Biol 19:701–706
11. Kyei GB, Dinkins C, Davis AS, Roberts E, Singh SB, Dong C et al (2009) Autophagy pathway intersects with HIV-1 biosynthesis and regulates viral yields in macrophages. J Cell Biol 186:255–268
12. Lenassi M, Cagney G, Liao M, Vaupotic T, Bartholomeeusen K, Cheng Y et al (2010) HIV Nef is secreted in exosomes and triggers apoptosis in bystander CD4$^+$ T cells. Traffic 11:110–122
13. Lewis MJ, Lee P, Ng HL, Yang OO (2012) Immune selection in vitro reveals human immunodeficiency virus type 1 Nef sequence motifs important for its immune evasion function in vivo. J Virol 86:7126–7135
14. Muthumani K, Choo AY, Hwang DS, Premkumar A, Dayes NS, Harris C et al (2005) HIV-1 Nef-induced FasL induction and bystander killing requires p38 MAPK activation. Blood 106:2059–2068
15. Muthumani K, Choo AY, Shedlock DJ, Laddy DJ, Sundaram SG, Hirao L et al (2008) Human immunodeficiency virus type 1 Nef induces programmed death 1 expression through a p38 mitogen-activated protein kinase-dependent mechanism. J Virol 82:11536–11544
16. Xu W, Santini PA, Sullivan JS, He B, Shan M, Ball SC et al (2009) HIV-1 evades virus-specific IgG2 and IgA responses by targeting systemic and intestinal B cells via long-range intercellular conduits. Nat Immunol 10:1008–1017
17. Aldrovandi GM, Gao L, Bristol G, Zack JA (1998) Regions of human immunodeficiency virus type 1 nef required for function in vivo. J Virol 72:7032–7039
18. Aldrovandi GM, Zack JA (1996) Replication and pathogenicity of human immunodeficiency virus type 1 accessory gene mutants in SCID-hu mice. J Virol 70:1505–1511
19. Duus KM, Miller ED, Smith JA, Kovalev GI, Su L (2001) Separation of human immunodeficiency virus type 1 replication from nef-mediated pathogenesis in the human thymus. J Virol 75:3916–3924
20. Fackler OT, Moris A, Tibroni N, Giese SI, Glass B, Schwartz O et al (2006) Functional characterization of HIV-1 Nef mutants in the context of viral infection. Virology 351:322–339
21. Glushakova S, Grivel JC, Suryanarayana K, Meylan P, Lifson JD, Desrosiers R et al (1999) Nef enhances human immunodeficiency virus replication and responsiveness to interleukin-2 in human lymphoid tissue ex vivo. J Virol 73:3968–3974
22. Glushakova S, Munch J, Carl S, Greenough TC, Sullivan JL, Margolis L et al (2001) CD4 down-modulation by human immunodeficiency virus type 1 Nef correlates with the efficiency of viral replication and with CD4(+) T-cell depletion in human lymphoid tissue ex vivo. J Virol 75:10113–10117
23. Homann S, Tibroni N, Baumann I, Sertel S, Keppler OT, Fackler OT (2009) Determinants in HIV-1 Nef for enhancement of virus replication and depletion of CD4+ T lymphocytes in human lymphoid tissue ex vivo. Retrovirology 6:6
24. Jamieson BD, Aldrovandi GM, Planelles V, Jowett JB, Gao L, Bloch LM et al (1994) Requirement of human immunodeficiency virus type 1 nef for in vivo replication and pathogenicity. J Virol 68:3478–3485
25. Schweighardt B, Roy AM, Meiklejohn DA, Grace EJ 2nd, Moretto WJ, Heymann JJ et al (2004) R5 human immunodeficiency virus type 1 (HIV-1) replicates more efficiently in primary CD4+ T-cell cultures than X4 HIV-1. J Virol 78:9164–9173
26. Stoddart CA, Geleziunas R, Ferrell S, Linquist-Stepps V, Moreno ME, Bare C et al (2003) Human immunodeficiency virus type 1 Nef-mediated downregulation of CD4 correlates with Nef enhancement of viral pathogenesis. J Virol 77:2124–2133
27. Denton PW, Estes JD, Sun Z, Othieno FA, Wei BL, Wege AK et al (2008) Antiretroviral pre-exposure prophylaxis prevents vaginal transmission of HIV-1 in humanized BLT mice. PLoS Med 5:e16
28. Nie C, Sato K, Misawa N, Kitayama H, Fujino H, Hiramatsu H et al (2009) Selective infection of CD4+ effector memory T lymphocytes leads to preferential depletion of memory T lymphocytes in R5 HIV-1-infected humanized NOD/SCID/IL-2Rgammanull mice. Virology 394:64–72
29. Dudek TE, No DC, Seung E, Vrbanac VD, Fadda L, Bhoumik P et al (2012) Rapid evolution of HIV-1 to functional CD8+ T cell responses in humanized BLT mice. Sci Transl Med 4:143ra198
30. Long BR, Stoddart CA (2012) Alpha interferon and HIV infection cause activation of human T cells in NSG-BLT mice. J Virol 86:3327–3336
31. Rhodes DI, Ashton L, Solomon A, Carr A, Cooper D, Kaldor J et al (2000) Characterization of three nef-defective human immunodeficiency virus type 1 strains associated with long-term nonprogression. Australian Long-Term Nonprogressor Study Group. J Virol 74:10581–10588
32. Zou W, Denton PW, Watkins RL, Krisko JF, Nochi T, Foster JL et al (2012) Nef functions in BLT mice to enhance HIV-1 replication and deplete CD4+CD8+ thymocytes. Retrovirology 9:44
33. Krisko JF, Martinez-Torres F, Foster JL, Garcia JV (2013) HIV restriction by APOBEC3 in humanized mice. PLoS Pathog 9:e1003242
34. Leslie A, Matthews PC, Listgarten J, Carlson JM, Kadie C, Ndung'u T et al (2010) Additive contribution of HLA class I alleles in the immune control of HIV-1 infection. J Virol 84:9879–9888
35. Usami Y, Gottlinger H (2013) HIV-1 Nef responsiveness is determined by Env variable regions involved in trimer association and correlates with neutralization sensitivity. Cell Rep 5:802–812
36. Choudhary SK, Walker RM, Powell DM, Planelles V, Walsh C, Camerini D (2006) CXCR4 tropic human immunodeficiency virus type 1 induces an apoptotic cascade in immature infected thymocytes that resembles thymocyte negative selection. Virology 352:268–284

37. Finkel TH, Tudor-Williams G, Banda NK, Cotton MF, Curiel T, Monks C et al (1995) Apoptosis occurs predominantly in bystander cells and not in productively infected cells of HIV- and SIV-infected lymph nodes. Nat Med 1:129–134
38. Geleziunas R, Xu W, Takeda K, Ichijo H, Greene WC (2001) HIV-1 Nef inhibits ASK1-dependent death signalling providing a potential mechanism for protecting the infected host cell. Nature 410:834–838
39. Grivel JC, Malkevitch N, Margolis L (2000) Human immunodeficiency virus type 1 induces apoptosis in CD4(+) but not in CD8(+) T cells in ex vivo-infected human lymphoid tissue. J Virol 74:8077–8084
40. Doitsh G, Cavrois M, Lassen KG, Zepeda O, Yang Z, Santiago ML et al (2010) Abortive HIV infection mediates CD4 T cell depletion and inflammation in human lymphoid tissue. Cell 143:789–801
41. Doitsh G, Galloway NL, Geng X, Yang Z, Monroe KM, Zepeda O et al (2014) Cell death by pyroptosis drives CD4 T-cell depletion in HIV-1 infection. Nature 505:509–514
42. Garg H, Mohl J, Joshi A (2012) HIV-1 induced bystander apoptosis. Viruses 4:3020–3043
43. Murooka TT, Deruaz M, Marangoni F, Vrbanac VD, Seung E, von Andrian UH et al (2012) HIV-infected T cells are migratory vehicles for viral dissemination. Nature 490:283–287
44. Arora VK, Molina RP, Foster JL, Blakemore JL, Chernoff J, Fredericksen BL et al (2000) Lentivirus Nef specifically activates Pak2. J Virol 74:11081–11087
45. Rauch S, Pulkkinen K, Saksela K, Fackler OT (2008) Human immunodeficiency virus type 1 Nef recruits the guanine exchange factor Vav1 via an unexpected interface into plasma membrane microdomains for association with p21-activated kinase 2 activity. J Virol 82:2918–2929
46. Dyer WB, Zaunders JJ, Yuan FF, Wang B, Learmont JC, Geczy AF et al (2008) Mechanisms of HIV non-progression; robust and sustained CD4+ T-cell proliferative responses to p24 antigen correlate with control of viraemia and lack of disease progression after long-term transfusion-acquired HIV-1 infection. Retrovirology 5:112
47. Zaunders J, Dyer WB, Churchill M (2011) The Sydney blood bank cohort: implications for viral fitness as a cause of elite control. Curr Opin HIV AIDS 6:151–156
48. Denton PW, Krisko JF, Powell DA, Mathias M, Kwak YT, Martinez-Torres F et al (2010) Systemic administration of antiretrovirals prior to exposure prevents rectal and intravenous HIV-1 transmission in humanized BLT mice. PLoS One 5:e8829
49. Denton PW, Olesen R, Choudhary SK, Archin NM, Wahl A, Swanson MD et al (2012) Generation of HIV latency in humanized BLT mice. J Virol 86:630–634
50. Denton PW, Othieno F, Martinez-Torres F, Zou W, Krisko JF, Fleming E et al (2011) One percent tenofovir applied topically to humanized BLT mice and used according to the CAPRISA 004 experimental design demonstrates partial protection from vaginal HIV infection, validating the BLT model for evaluation of new microbicide candidates. J Virol 85:7582–7593
51. Kim SS, Peer D, Kumar P, Subramanya S, Wu H, Asthana D et al (2010) RNAi-mediated CCR5 silencing by LFA-1-targeted nanoparticles prevents HIV infection in BLT mice. Mol Ther 18:370–376
52. Lan P, Tonomura N, Shimizu A, Wang S, Yang YG (2006) Reconstitution of a functional human immune system in immunodeficient mice through combined human fetal thymus/liver and CD34+ cell transplantation. Blood 108:487–492
53. Melkus MW, Estes JD, Padgett-Thomas A, Gatlin J, Denton PW, Othieno FA et al (2006) Humanized mice mount specific adaptive and innate immune responses to EBV and TSST-1. Nat Med 12:1316–1322
54. Rajesh D, Zhou Y, Jankowska-Gan E, Roenneburg DA, Dart ML, Torrealba J et al (2010) Th1 and Th17 immunocompetence in humanized NOD/SCID/IL2rgammanull mice. Hum Immunol 71:551–559
55. Sun Z, Denton PW, Estes JD, Othieno FA, Wei BL, Wege AK et al (2007) Intrarectal transmission, systemic infection, and CD4+ T cell depletion in humanized mice infected with HIV-1. J Exp Med 204:705–714
56. Koyanagi Y, Miles S, Mitsuyasu RT, Merrill JE, Vinters HV, Chen IS (1987) Dual infection of the central nervous system by AIDS viruses with distinct cellular tropisms. Science 236:819–822
57. Wei BL, Denton PW, O'Neill E, Luo T, Foster JL, Garcia JV (2005) Inhibition of lysosome and proteasome function enhances human immunodeficiency virus type 1 infection. J Virol 79:5705–5712
58. Palmer S, Wiegand AP, Maldarelli F, Bazmi H, Mican JM, Polis M et al (2003) New real-time reverse transcriptase-initiated PCR assay with single-copy sensitivity for human immunodeficiency virus type 1 RNA in plasma. J Clin Microbiol 41:4531–4536
59. Denton PW, Garcia JV (2012) Mucosal HIV-1 transmission and prevention strategies in BLT humanized mice. Trends Microbiol 20:268–274